

system. Recent work in our laboratory has now established the formation of the epoxide in the O-C₃F₆-O₂ system. The rate constant ratio $k_m/k_o^{1/2}$ is 0.05 (l./mole sec)^{1/2} for the C₂F₄ system compared to 0.068 (l./mole sec)^{1/2} for the analogous ratio in the C₃F₆ system.

Acknowledgment. The authors wish to thank Mr. Dennis Saunders for preparation of the C₂F₄ and Drs. Caglioti, Lenzi, and Mele for access to their original infrared spectrum of C₂F₄O. They also wish to thank Mrs. Barbara Peer and Miss Jeanne Kiley for assistance with the manuscript.

A Reexamination of the Mercury-Photosensitized Oxidation of Tetrafluoroethylene

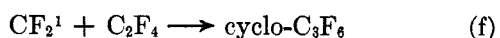
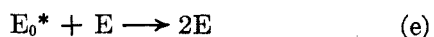
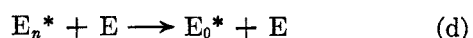
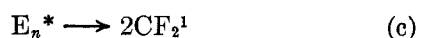
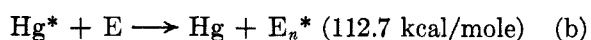
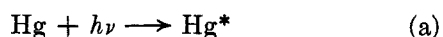
by Julian Heicklen and Vester Knight

Aerospace Corporation, El Segundo, California (Received June 20, 1966)

The mercury-photosensitized oxidation of C₂F₄ was studied at 29 and 127°. The absorbed intensity was varied by a factor of 1000, and the O₂ and C₂F₄ pressures by a factor of 30. The products of the reaction were cyclo-C₃F₆, CF₂O, and C₂F₄O (tetrafluoroethylene oxide). Important intermediates in the oxidation are an electronically excited C₂F₄ molecule and the CF₂O₂ radical. In addition, both singlet and triplet CF₂ radicals are involved. A detailed reaction mechanism is presented, and several rate constant ratios are obtained. Where comparisons with literature values could be made, agreement is good. The important oxidation step that generates the CF₂O₂ radicals is E₀* + O₂ → CF₂O₂ + CF₂¹, where E₀* is a vibrationally equilibrated electronically excited C₂F₄ molecule, and CF₂¹ is the singlet CF₂ radical.

I. Introduction

The mercury-sensitized photolysis of C₂F₄ has been studied previously, both in the absence of O₂¹⁻³ and in the presence of O₂.² In the absence of O₂, the mechanism has been reasonably well established to be



where E is C₂F₄, the asterisk represents an electronically excited molecule (surely a triplet), the subscript *n* represents vibrational excitation, and the subscript 0 represents vibrationally unexcited molecules. The CF₂ radicals formed are in the singlet state, which is shown by the superscript 1. That the singlet CF₂ is formed was indicated in the oxidation studies where the results excluded the possibility of CF₂ radicals reacting with O₂. However, with oxygen present, oxidation products were formed from the oxidation of the electronically excited C₂F₄. In the absence of O₂,

(1) B. Atkinson, *J. Chem. Soc.*, 2684 (1952).

(2) J. Heicklen, V. Knight, and S. A. Greene, *J. Chem. Phys.*, **42**, 221 (1965).

(3) N. Cohen and J. Heicklen, *ibid.*, **43**, 871 (1965).

Table I: Results of Photolyses at 29°

(C ₂ F ₄), mm	(O ₂), mm	Φ(CF ₂ O)	Φ(C ₂ F ₄ O)	Φ(cyclo- C ₃ F ₄)	α	β	γ	ψ
<i>I_a</i> = 17.9 μ/sec (Aerospace C ₂ F ₄)								
9.5	0.0	0.0022
16	0.0	0.0028
17	16	...	0.003	...	0.077	0.77	0.58	0.54
29	0.0	0.0069
53	0.0	0.0077
54	16	0.30	0.050	...	0.21	0.92	0.54	0.42
147	16	0.30	...	0.026	0.42	0.97	0.55	0.32
169	17	...	0.110	...	0.46	0.97	0.56	0.32
152	51	0.40	0.43	0.97	0.70	0.56
164	151	...	0.088	...	0.45	0.97	0.83	0.76
325	16	0.038	0.62	0.99	0.67	0.255
440	15	0.65	0.074	0.096	0.69	0.99	0.80	0.191
<i>I_a</i> = 7.8 μ/sec (Peninsular C ₂ F ₄)								
15	0.0	0.0056
16	16	0.76, 0.63	0.047	0.0035	0.074	0.76	0.58	0.54
				0.0028				
49	0.0	0.0120
53	16	0.48	...	0.0097	0.21	0.92	0.54	0.42
				0.0187				
64	16	0.48	0.24	0.93	0.52	0.40
50	64	...	0.076	0.0116	0.20	0.92	0.77	0.73
149	0.0	0.033
153	16	0.32, 0.42	0.107	...	0.43	0.97	0.56	0.31
156	52	0.44, 0.44	...	0.037	0.44	0.97	0.70	0.56
180	50	...	0.158	...	0.47	0.97	0.70	0.54
115	175	...	0.22	...	0.36	0.96	0.84	0.81
140	166	0.69	~0.23	0.032	0.41	0.97	0.84	0.80
445	0.0	0.073
455	4.5	0.146	0.70	0.99	0.71	0.079
410	15	0.093	0.67	0.99	0.70	0.22
465	16	0.21, 0.22	0.092	0.079	0.70	0.99	0.72	0.217
465	52	0.40	0.160	0.091	0.70	0.99	0.76	0.45
395	152	0.081	0.66	0.99	0.76	0.62
465	150	0.73	0.25, 0.26	0.099	0.70	0.99	0.84	0.67
<i>I_a</i> = 4.0 μ/sec (Aerospace C ₂ F ₄)								
19	16	...	~0.016	...	0.087	0.79	0.58	0.53
65	16	0.67	0.040	...	0.245	0.93	0.53	0.40
138	16	0.86, 1.05	0.20	...	0.41	0.97	0.54	0.32
168	50	0.88	0.143	...	0.46	0.97	0.70	0.55
147	130	0.031	0.42	0.97	0.86	0.79
149	158	...	0.078	...	0.43	0.97	0.84	0.78
150	185	0.40	0.43	0.97	0.85	0.80
300	17	0.174	0.60	0.99	0.66	0.27
375	17	...	0.26	...	0.65	0.99	0.68	0.245
<i>I_a</i> = 2.1 μ/sec (Peninsular C ₂ F ₄)								
17	0.0	0.0086
16	16	0.55	0.076	...	0.074	0.76	0.58	0.54
47	0.0	0.0246
50	65	0.55	0.114	...	0.20	0.92	0.77	0.70
149	0.0	0.046
164	17	0.41	0.092	...	0.45	0.97	0.56	0.33
170	52	0.57	0.174	...	0.46	0.97	0.70	0.55
148	159	0.72	0.197	...	0.43	0.97	0.84	0.78
504	0.0	0.128

(C ₂ F ₄), mm	(O ₂), mm	Φ(CF ₂ O)	Φ(C ₂ F ₄ O)	Φ(cyclo- C ₃ F ₆)	α	β	γ	ψ
475	16	0.21	0.72	0.99	0.72	0.214
490	18	0.33	0.093	...	0.71	0.99	0.73	0.23
482	51	0.47	0.162	...	0.71	0.99	0.78	0.44
502	50	0.53	0.21	...	0.72	0.99	0.78	0.44
480	148	0.79	0.26	...	0.71	0.99	0.84	0.66
491	150	0.78	0.32	...	0.71	0.99	0.81	0.64
<i>I_a</i> = 0.91 μ/sec (Aerospace C ₂ F ₄)								
17	18	0.82	0.078	0.77	0.60	0.56
58	18	0.89	0.032	0.041	0.225	0.92	0.55	0.44
150	17	1.30	0.28	0.119	0.43	0.97	0.56	0.33
136	51	...	0.32	0.061	0.40	0.97	0.70	0.58
163	51	1.43	0.45	0.97	0.70	0.58
151	163	1.71	0.48	0.107	0.43	0.97	0.84	0.78
430	17	0.38	0.68	0.99	0.72	0.236
<i>I_a</i> = 0.142 μ/sec (Peninsular C ₂ F ₄)								
150	0.0	0.23, 0.23
158	15	0.61, 0.64	0.27	0.26	0.44	0.97	0.55	0.30
150	164	1.51	0.57	0.20	0.43	0.97	0.84	0.78
510	0.0	0.55
432	16	0.75	0.35	...	0.68	0.99	0.72	0.226
467	15	0.51	...	0.55	0.70	0.99	0.72	0.21
485	150	2.6	0.73	0.55	0.71	0.99	0.84	0.67
<i>I_a</i> = 0.041 μ/sec (Peninsular C ₂ F ₄)								
477	0.0	0.66
468	150	2.7	0.61	0.56	0.70	0.99	0.84	0.67
<i>I_a</i> = 0.018 ± 0.008 μ/sec (Peninsular C ₂ F ₄)								
505	0.0	0.42
511	150	2.6	...	0.35	0.72	0.99	0.84	0.56

the fate of E₀* was not ascertained, though ultimately it must return to ground-state C₂F₄. The deactivation could either be by collision or by a first-order process. We anticipate the results of this study and write the deactivation step e as a collision-induced transition.

In the previous oxidation study, the products were found to be cyclo-C₃F₆, CF₂O, and an unidentified product with infrared absorption bands at 6.22 and 8.85 μ. This product has since been shown to be tetrafluoroethylene oxide (C₂F₄O).⁴ The analyses were performed by gas chromatography after the oxidation products had been converted to CO₂. Thus, products were reported as cyclo-C₃F₆ and CO₂. In the study reported in the present paper, analyses were made continuously during a run for each of the products by *in situ* infrared analysis. In the previous study, the C₂F₄ pressure was varied from 0.6 to 60 mm, the intensity by a factor of 5, and the temperature not at all. In the present study, the C₂F₄ pressure was varied from 15 to 500 mm, and the intensity by a factor of 10³. Furthermore, runs were made at both 29 and 127°.

II. Experimental Section

Matheson Co. N₂O and O₂ were used. The O₂ was not further purified, but the N₂O was degassed at -196° before use. Two samples of C₂F₄ were used. One was obtained from Peninsular ChemResearch, Inc., and was purified by collecting only that fraction volatile at -126° and condensable at -196°. The other sample was prepared in our laboratory by the debromination of vicinal dibromide C₂F₄Br₂ (E. I. du Pont de Nemours, Freon 114-B-2). The liquid Freon was added dropwise to a warm (50°) slurry of zinc dust and methanol containing some ZnCl₂. The rate of addition was adjusted to keep the solvent gently refluxing, and the effluent C₂F₄ was subsequently purified by passing it through water, through Drierite, and then through silica gel. Finally, it was degassed at -196°. Analyses of both samples of C₂F₄ were performed using a Beckman GC-2A programmed-temperature gas

(4) V. Caglioti, M. Lenzi, and A. Mele, *Nature*, 201, 610 (1964).

Table II: Results of Photolyses at 127°^a

(C ₂ F ₄), mm	(O ₂), mm	Φ(CF ₂ O)	Φ(C ₂ F ₄ O)	Φ(cyclo- C ₃ F ₆)	α	β	γ	ψ
<i>I_a</i> = 18.2 μ/sec								
15	0.0	0.029
18	15	0.70	0.073	0.025	0.083	0.78	0.57	0.52
51	0.0	0.044
50	15	1.12	0.129	...	0.20	0.91	0.52	0.41
65	16	0.063	0.245	0.93	0.52	0.42
153	0.0	0.079
140	16	...	0.24	0.095	0.41	0.97	0.54	0.32
156	15	0.97	0.44	0.97	0.55	0.30
140	55	...	0.28	...	0.41	0.97	0.71	0.59
162	50	1.40	...	0.096	0.45	0.97	0.70	0.55
150	154	1.65	0.38	...	0.43	0.97	0.84	0.77
148	170	0.102	0.42	0.97	0.84	0.80
503	0.0	0.135
503	17	...	0.24	0.21	0.72	0.99	0.76	0.224
551	15	0.81	0.73	0.99	0.76	0.193
400	150	1.68	0.67	0.99	0.84	0.69
465	150	...	0.46	0.154	0.70	0.99	0.84	0.67
<i>I_a</i> = 3.4 μ/sec								
17	0.0	0.056
16	18	1.02	0.111	0.040	0.074	0.76	0.60	0.56
51	0.0	0.104
55	15	1.46	0.30	0.121	0.216	0.92	0.54	0.42
150	0.0	0.191
155	16	1.20	0.34	0.22	0.44	0.97	0.56	0.31
152	52	1.95	0.53	0.20	0.43	0.97	0.70	0.57
150	148	2.42	0.64	...	0.43	0.97	0.82	0.76
150	170	0.20	0.43	0.97	0.84	0.79
485	0.0	0.38
489	17	0.75	0.28	0.40	0.71	0.99	0.74	0.22
487	150	2.15	0.75	0.35	0.71	0.99	0.84	0.66

^a Peninsular C₂F₄ used in all runs.

chromatograph utilizing a silica gel column. Both samples showed less than 0.1% of any impurity.

The vacuum manifold, T-shaped cell, and the optical arrangement have been described previously.⁵⁻⁸ The infrared analyses were performed *in situ* in a Perkin-Elmer Model 13 Universal spectrometer. Both the stem and the cross of the T-shaped cell were 10 cm long and 5 cm in diameter. Irradiation was from a Hanovia low-pressure, spiral mercury lamp. The radiation passed through a Corning 9-54 filter (to remove radiation below 2200 Å), through 0-10 Corning 9-30 filters (to reduce the intensity), and through a quartz window on the stem of the cell. The cross of the T had NaCl windows and was situated in the sample beam of the infrared spectrometer. During any irradiation, only one product band was followed, and it was followed continuously.

The infrared bands and extinction coefficients used for analysis were the same used previously.⁸ Absolute

intensities were measured continually by following CF₂O production in separate experiments of the mercury-sensitized photolysis of 500 mm of N₂O in the presence of 30 mm of C₂F₄. Under these conditions, Φ(CF₂O) is equal to 1.00.^{5,7}

III. Results

As in the previous studies,¹⁻³ the products were found to be cyclo-C₃F₆ in the absence of O₂, and cyclo-C₃F₆, CF₂O, and C₂F₄O (tetrafluoroethylene oxide) in the presence of O₂. In the absence of O₂, the cyclo-C₃F₆ grew linearly with exposure time. However, in the presence of O₂, the rates of growth of the products

(5) D. Saunders and J. Heicklen, *J. Am. Chem. Soc.*, **87**, 2088 (1965).

(6) D. Marsh and J. Heicklen, *J. Phys. Chem.*, **69**, 4410 (1965).

(7) D. Saunders and J. Heicklen, Report No. TDR-669(6250-40)-3, Vol. I, Aerospace Corp., Jan 1966; *J. Phys. Chem.*, **70**, 1950 (1966).

(8) J. Heicklen and V. Knight, *ibid.*, **70**, 3893 (1966).

(C ₂ F ₄), mm	(O ₂), mm	Φ(CF ₂ O)	Φ(C ₂ F ₄ O)	Φ(cyclo- C ₃ F ₆)	α	β	γ	ψ
$I_a = 0.64 \mu/\text{sec}$								
15	0.0	0.131
16	17	0.99	0.099	0.102	0.074	0.76	0.59	0.56
51	0.0	0.23
45	15	1.83	0.184	0.90	0.52	0.42
60	17	...	0.39	0.28	0.23	0.92	0.54	0.42
150	0.0	0.37
141	15	1.24	0.41	0.97	0.54	0.30
158	18	...	0.41	0.46	0.44	0.97	0.56	0.33
154	51	2.22	0.43	0.97	0.70	0.56
166	51	...	0.52	0.46	0.45	0.97	0.70	0.56
151	162	2.70	0.71	0.40	0.43	0.97	0.84	0.79
460	0.0	0.63
480	16	1.21	0.47	0.68	0.71	0.99	0.74	0.22
482	151	2.22	0.99	0.67	0.71	0.99	0.84	0.68
$I_a = 0.24 \mu/\text{sec}$								
15	0.0	0.160
16	16	...	0.21	0.102	0.074	0.76	0.58	0.53
15	18	0.81	0.070	0.75	0.60	0.56
53	0.0	0.31
57	17	0.93, 0.95	0.20	0.26	0.222	0.92	0.54	0.42
151	0.0	0.35
150	16	0.91	0.34	...	0.43	0.97	0.56	0.32
174	16	0.35	0.47	0.97	0.58	0.31
160	51	...	0.42	0.38	0.44	0.97	0.54	0.44
199	51	1.26	0.50	0.97	0.71	0.54
150	158	1.78	0.54	0.29	0.43	0.97	0.84	0.78
465	0.0	0.44
480	16	1.14	0.54	0.46	0.71	0.99	0.74	0.215
498	150	2.6	0.90	0.57	0.71	0.99	0.84	0.67

were not constant. At room temperature, there was a mild inhibition of all product formation as irradiation continued. This effect became more pronounced as the (O₂)/(C₂F₄) ratio increased. At 127°, there was a mild acceleration of CF₂O and cyclo-C₃F₆ formation and a mild inhibition of C₂F₄O formation. However, the effect was not nearly as large as found in another system.⁸ After irradiation at 127°, the C₂F₄O slowly disappeared.

The initial quantum yields of product formation are given in Tables I and II. Double entries indicate the results of duplicate runs. The variation of the yields is a complex function of temperature, intensity, and reactant pressures. Nevertheless, the over-all trends can be summarized as follows.

First, Φ(cyclo-C₃F₆) is nearly unaffected by the presence of O₂, but it does rise by enhancing the C₂F₄ pressure or diminishing the intensity. For comparable conditions, Φ(cyclo-C₃F₆) is larger at the higher tem-

perature, but the upper limit is about 0.6 at both temperatures.

Second, Φ(CF₂O) is always greater than Φ(C₂F₄O), and neither is markedly affected by a change in temperature.

Third, Φ(CF₂O) rises from about 0.2 to 2.7 and Φ(C₂F₄O) rises from about 0.003 to 1.0 as either the C₂F₄ pressure is increased or the absorbed intensity is decreased.

Fourth, for constant (C₂F₄) and I_a, both Φ(CF₂O) and Φ(C₂F₄O) rise measurably as the O₂ pressure is raised.

IV. Discussion

In the absence of O₂, the mechanism is given by reactions a through g. A steady-state analysis leads to the following predictions. For large (C₂F₄)[1 + (k_d/k_c)(C₂F₄)]^{1/2}/I_a^{1/2} where R(f) > R(g) we have

$$\Phi(\text{cyclo-C}_3\text{F}_6) \left[1 + \frac{k_d}{k_c} (\text{C}_2\text{F}_4) \right] = 2.0 \quad (1)$$

For small $(\text{C}_2\text{F}_4) [1 + (k_d/k_c)(\text{C}_2\text{F}_4)]^{1/2}/I_a^{1/2}$ where $R(f) < R(g)$

$$\Phi(\text{cyclo-C}_3\text{F}_6) \left[1 + \frac{k_d}{k_c} (\text{C}_2\text{F}_4) \right] = \frac{k_f}{k_g^{1/2} (\text{C}_2\text{F}_4)} \frac{[1 + (k_d/k_c)(\text{C}_2\text{F}_4)]^{1/2}}{I_a^{1/2}} \quad (2)$$

where $R(X)$ is the rate of reaction X , $\Phi(X)$ is the quantum yield of production of X , and I_a is the absorbed intensity. The rate constant ratio k_d/k_c can be estimated from eq 1 and the fact that the upper limiting value of $\Phi(\text{cyclo-C}_3\text{F}_6)$ is 0.6 with 500 mm of C_2F_4 at both temperatures. Thus, k_d/k_c is found to be $5 \times 10^{-3} \text{ mm}^{-1}$, which is in good agreement with an earlier estimate of $4 \times 10^{-3} \text{ mm}^{-1}$ at 175° .³ Using the value of $5 \times 10^{-3} \text{ mm}^{-1}$ for k_d/k_c permits us to calculate the quantities on both sides of eq 2 from the data in Tables I and II. For the runs in the absence of O_2 , the appropriate quantities are plotted in Figure 1. For low values of the coordinates, the log-log plots are linear with slope unity at both temperatures. However, the intercept is higher at the elevated temperature. For large values of the abscissa, the ordinate levels off at 2.0. Thus, the predictions of eq 1 and 2 are fulfilled.

Comparable studies have been made previously,^{3,9} and those results are indicated in Figure 1 by solid lines. Saunders' experiments were performed in an X-shaped cell at 24° , and the results agree exactly with ours. On the other hand, Cohen and Heicklen's experiments were performed in a cylindrical cell, and the results lie above ours at both temperatures. The apparent discrepancy is easily explained because the abscissa is an intensity-dependent function. In our calculations, we have assumed a uniform intensity throughout the cell, when in fact the ultraviolet radiation was absorbed nonuniformly in the stem of the T-shaped cell. Therefore, the effective absorbed intensity in Saunders' and in our experiments was greater than the average intensity, and the points lie below those of Cohen and Heicklen. A further corroboration of this point is achieved from a careful examination of the data points. The points at the higher pressures (where diffusion is slower and the effective absorbed intensity is larger) lie slightly below the straight-line extension of those at lower pressures. The more accurate value of $k_f/k_g^{1/2}$ is that obtained from Cohen and Heicklen's data where the radical concentration is more nearly uniform; even those values may be slightly low.

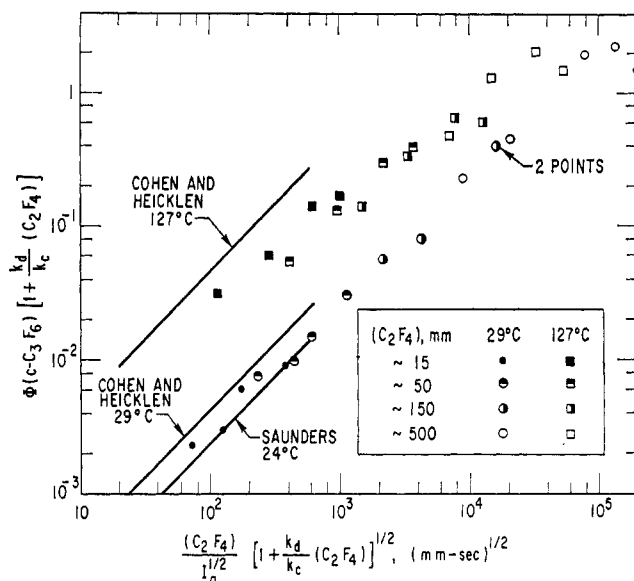
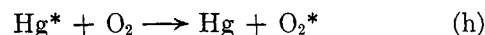


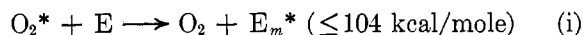
Figure 1. Log-log plots of $\Phi(\text{cyclo-C}_3\text{F}_6)[1 + (k_d/k_c)(\text{C}_2\text{F}_4)]$ in the absence of O_2 vs. $(\text{C}_2\text{F}_4) \times [1 + (k_d/k_c)(\text{C}_2\text{F}_4)]^{1/2}/I_a^{1/2}$ at 29 and 127° .

In the presence of O_2 , additional reactions occur. In the first place, the excited mercury atom can transfer its energy to O_2



A summary of all the evidence indicates that O_2^* is the $c^1\Sigma_u^-$ electronic state of O_2 .¹⁰ The excited molecule must contain sufficient energy to react with an unexcited O_2 and produce O_3 and oxygen atoms some of the time. Furthermore, the spin conservation rules predict that a singlet level be formed. The $c^1\Sigma_u^-$ state is the only state that meets both requirements. Additional supporting evidence has been obtained in this laboratory,^{11,12} where it has been shown that O_2^* transfers its energy to C_3F_6 to form an electronically excited molecule (presumably a triplet). The spin rules and energetic considerations favor the $c^1\Sigma_u^-$ state for O_2^* . The present study with C_2F_4 further supports this hypothesis.

The electronically excited oxygen can transfer its energy to C_2F_4



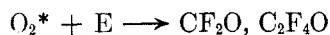
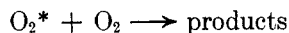
where the subscript m refers to less vibrational energy than the subscript n . Two other reactions of O_2^* are possible

(9) D. Saunders, unpublished work of this laboratory, 1964.

(10) D. Volman, *Advan. Photochem.*, **1**, 43 (1963).

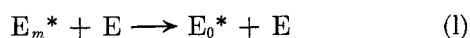
(11) J. Heicklen and V. Knight, *J. Phys. Chem.*, **69**, 3641 (1965).

(12) J. Heicklen and T. Johnston, to be published.



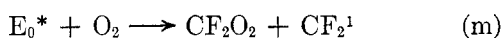
In these studies we kept the $(\text{O}_2)/(\text{C}_2\text{F}_4)$ ratio below unity. Under these conditions, the results of ref 2 indicate that the first reaction is negligible compared to reaction i. The second reaction cannot be important, for if it were, the rates of formation of the oxidation products would not fall off with diminishing C_2F_4 pressure. The results of ref 2 clearly establish the falloff.

The initially formed vibronically excited molecule behaves like E_n^*

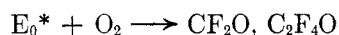


For both reactions d and l, O_2 has been excluded as a deactivating gas for simplicity. Such a simplification is justified because $(\text{O}_2)/(\text{C}_2\text{F}_4)$ was kept below unity, and O_2 is surely a much less efficient deactivator than C_2F_4 .

The vibrationally inactive molecule E_0^* can react with oxygen

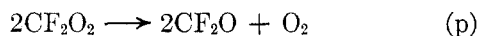
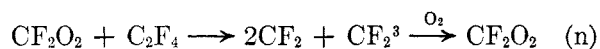


Reaction m must produce singlet CF_2 radicals in order to keep the cyclo- C_3F_6 yield from falling in the presence of O_2 . Triplet CF_2 radicals would be scavenged by O_2 ,¹³ and are thus ruled out. The alternate reaction

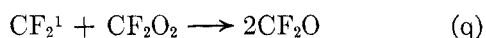


may play some role, but it cannot be important. If it were, $\Phi(\text{cyclo-C}_3\text{F}_6)$ should fall markedly when O_2 is added, contrary to fact.

The CF_2O_2 radicals have been shown to react *via*⁸



Under our conditions here, where (O_2) is greater than 15 mm, the triplet CF_2 radicals are always scavenged by O_2 .⁸ Two other reactions that need to be considered in this system are



The oxidation mechanism predicts that

$$\theta = \frac{k_j}{k_1}(\text{E})^{-1} \quad (3)$$

where θ is defined as

$$\theta \equiv \left\{ \left[\Phi(\text{CF}_2\text{O}) - \frac{2k_n}{k_o} \Phi(\text{C}_2\text{F}_4\text{O}) \right] \left[1 + \frac{k_h}{k_b} \frac{(\text{O}_2)}{(\text{E})} \right] \times \left[1 + \frac{k_e(\text{E})}{k_m(\text{O}_2)} \right] - \alpha \right\}^{-1} \frac{k_h}{k_b} \frac{(\text{O}_2)}{(\text{E})} - 1 \quad (4)$$

The quantity α is the fraction of E_n^* which is deactivated to E_0^* and is

$$\alpha \equiv \frac{k_d(\text{E})/k_c}{1 + k_d(\text{E})/k_c} \quad (5)$$

It can be calculated from the known value of k_d/k_c of $5 \times 10^{-3} \text{ mm}^{-1}$, and the values are listed in Tables I and II. The ratio k_h/k_b can be obtained from data already in the literature. The ratio of the rate constants for Hg^* quenching by O_2 and N_2O has been found to be 1.00 by Yarwood, Strausz, and Gunning,¹⁴ although Calvert and Pitts¹⁵ report a value of 1.26. The relative rate constants for Hg^* quenching by C_2F_4 and N_2O have been reported to be 0.31,⁵ 0.35,¹⁶ 0.36,¹⁷ and 0.43.¹⁸ We use 1.00 and 0.35, respectively, for the two ratios and obtain a value of k_h/k_b of 2.8. The value for k_e/k_m is more elusive. However, by fitting our data, we estimate an approximate value of 0.08.

For the data obtained in this study, it is necessary to subtract two similar numbers to obtain θ . Thus, the errors are very large. However, in the work of ref 2 at low C_2F_4 pressures, more accurate values can be obtained for θ . Furthermore, in that work a number of simplifications exist: α is negligibly small; $k_h(\text{O}_2)/k_b(\text{E}) \gg 1.0$; $k_e(\text{E})/k_m(\text{O}_2) \ll 1.0$; and $\Phi(\text{C}_2\text{F}_4\text{O}) \ll \Phi(\text{CF}_2\text{O})$. The analytical scheme used in that work quantitatively converted the oxidation products to CO_2 . Since $\Phi(\text{C}_2\text{F}_4\text{O}) \ll \Phi(\text{CF}_2\text{O})$, the CO_2 production can be equated with CF_2O production, and eq 3 reduces to

$$[\Phi(\text{CO}_2)]^{-1} - 1 = \frac{k_j}{k_1}(\text{E})^{-1} \quad (6)$$

In the Hecklen, Knight, and Greene study,² quantum

(13) J. Hecklen, N. Cohen, and D. Saunders, *J. Phys. Chem.*, **69**, 1774 (1965).

(14) A. J. Yarwood, O. P. Strausz, and H. E. Gunning, *J. Chem. Phys.*, **41**, 1705 (1964).

(15) J. G. Calvert and J. N. Pitts, Jr., "Photochemistry," John Wiley and Sons, Inc., New York, N. Y., 1966, p 74.

(16) B. de B. Darwent, M. K. Phibbs, and F. G. Hurtubise, *J. Chem. Phys.*, **22**, 859 (1954).

(17) M. G. Bellas, Y. Rousseau, O. P. Strausz, and H. E. Gunning, *ibid.*, **41**, 768 (1964), as quoted in ref 14.

(18) A. R. Trobridge and K. R. Jennings, *Proc. Chem. Soc.*, 335 (1964).

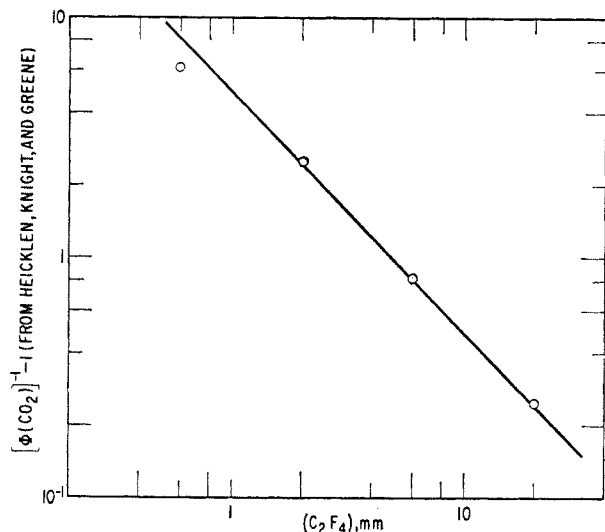


Figure 2. Log-log plot of $[\Phi(\text{CO}_2)]^{-1} - 1$ vs. (C_2F_4) at 23° .

yields were not reported because the absorbed intensity was not known. With 60 mm of C_2F_4 and excess O_2 , $\Phi(\text{CF}_2\text{O})$ should be near unity. Thus if we assume $\Phi(\text{CO}_2)$ is 1.2 (to allow for some $\text{C}_2\text{F}_4\text{O}$ formation), then the absorbed intensity and the quantum yield can be calculated. To check this assumption, this value of I_a and the rates of cyclo- C_3F_6 formation were used to calculate $k_f/k_g^{1/2}$. The value thus obtained corresponds exactly to that from this study.

Figure 2 is a plot of $[\Phi(\text{CO}_2)]^{-1} - 1$ vs. the C_2F_4 pressure based on the data of ref 2. The log-log plot is linear with a slope of -1.0 and yields a value of 5.0 mm of k_i/k_1 . The rate constants for energy removal k_d and k_1 probably correspond to the collision frequency and therefore are similar. Thus, k_c/k_i is about 40, a result to be expected since E_m^* has about 10 kcal/mole more energy than E_m^* .

From the rate constant information we now have, we can compute three more important quantities

$$\beta \equiv \frac{k_1(E)/k_j}{1 + k_1(E)/k_j} \quad (7)$$

$$\gamma \equiv \frac{\alpha + \beta k_h(\text{O}_2)/k_b(E)}{1 + k_h(\text{O}_2)/k_b(E)} \quad (8)$$

$$\psi \equiv \frac{\gamma}{1 + k_e(E)/k_m(\text{O}_2)} \quad (9)$$

where β is the fraction of E_m^* deactivated to E_0^* , γ is the quantum yield of E_0^* production, and ψ is the quantum yield of CF_2O_2 production. Values for these three quantities are listed in Tables I and II.

The quantum yield of production of CF_2^1 is $2(1 - \gamma) + \psi$, which is always larger than ψ , the quantum

yield of CF_2O_2 production. Therefore, when CF_2 radicals are removed primarily by radical-radical reactions, reaction g must play some role, no matter how fast reactions q and r are. For the pertinent conditions in our experiments, CF_2^1 is always produced at least 50% faster than CF_2O_2 , and in some cases, three times as fast. Thus, it is safe to make the simplification that CF_2^1 removal by reactions q and r is unimportant compared to removal by reaction g without introducing much error. A steady-state treatment leads to the following results: at high $(\text{C}_2\text{F}_4)/I_a^{1/2}(1 - \gamma + \psi/2)^{1/2}$ where $R(f) > R(g) + R(q) + R(r)$

$$\frac{\Phi(\text{cyclo-C}_3\text{F}_6)}{1 - \gamma + \psi/2} = 2.0 \quad (10)$$

At low $(\text{C}_2\text{F}_4)/I_a^{1/2}[1 - \gamma + \psi/2]^{1/2}$ where $R(g) > R(f)$

$$\frac{\Phi(\text{cyclo-C}_3\text{F}_6)}{1 - \gamma + \psi/2} = \frac{k_f}{k_g^{1/2}} \frac{(\text{C}_2\text{F}_4)}{I_a^{1/2}(1 - \gamma + \psi/2)^{1/2}} \quad [R(g) > R(q) + R(r)] \quad (11)$$

The appropriate quantities from eq 10 and 11 are plotted in Figure 3. Equations 10 and 11 are analogous to eq 1 and 2, respectively. For low values of the abscissa, the log-log plots should be linear with unit slope and an intercept of $k_f/k_g^{1/2}$, whereas at high values of the abscissa, the ordinate should approach 2.0. It is clear that Figure 3 follows the expected behavior. The lines that best fit the data points from Figure 1 in the absence of O_2 are shown in Figure 3. The remarkable agreement is gratifying.

Let us now consider the oxidation products. At high C_2F_4 pressures and low radical concentrations, CF_2O_2 is removed principally by reaction o, whereas for the reverse conditions, removal is primarily by reactions p, q, and r. Then the steady-state analysis leads to: at high $(\text{C}_2\text{F}_4)/(I_a\psi)^{1/2}$ or $(\text{C}_2\text{F}_4)/I_a^{1/2}(1 - \gamma + \psi/2)^{1/2}$, where $R(o) > R(p) + R(q) + R(r)$

$$\frac{\Phi(\text{CF}_2\text{O})}{\psi} = 1 + \frac{2k_n}{k_o} \quad (12)$$

$$\frac{\Phi(\text{C}_2\text{F}_4\text{O})}{\psi} = 1.0 \quad (13)$$

At low $(\text{C}_2\text{F}_4)/(I_a\psi)^{1/2}$, where $R(p) > R(o)$

$$\frac{\Phi(\text{CF}_2\text{O})}{\psi} = 1.0 \quad [R(p) > R(q) + R(r)] \quad (14)$$

$$\frac{\Phi(\text{C}_2\text{F}_4\text{O})}{\psi} = \frac{k_o}{(2k_p)^{1/2}} \frac{(\text{C}_2\text{F}_4)}{(I_a\psi)^{1/2}} \quad [R(p) > R(q) + R(r)] \quad (15)$$

At low $(\text{C}_2\text{F}_4)/I_a^{1/2}(1 - \gamma + \psi/2)^{1/2}$, where $R(q) + R(r) > R(o)$, we have relationships 16 and 17

$$\frac{\Phi(\text{CF}_2\text{O})}{\psi} = \frac{2k_q}{k_q + k_r} [R(q) + R(r) > R(p)] \quad (16)$$

$$\frac{\Phi(\text{C}_2\text{F}_4\text{O})}{\psi} = \frac{k_o k_g^{1/2}}{(k_q + k_r)} \frac{(\text{C}_2\text{F}_4)}{I_a^{1/2} (1 - \gamma + \psi/2)^{1/2}} [R(q) + R(r) > R(p)] \quad (17)$$

Equations 14 through 17 are all based on the already justified simplification that $R(g) > R(p)$. For eq 14 and 15, reactions q and r have been neglected in the steady-state assumption, whereas in eq 16 and 17, reaction p has been neglected in the steady-state assumption. It was necessary to do this to make the expressions tractable. As shall be seen, neither as-

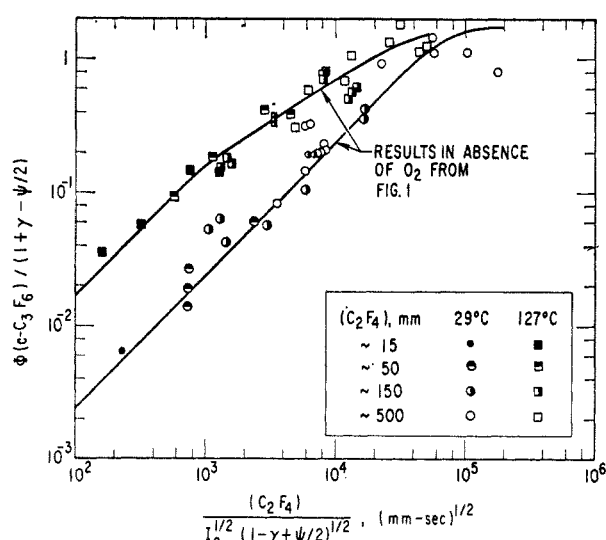


Figure 3. Log-log plots of $\Phi(\text{cyclo-C}_3\text{F}_6)/(1 + \gamma - \psi/2)$ in the presence of O_2 vs. $(\text{C}_2\text{F}_4)/I_a^{1/2} \times (1 - \gamma + \psi/2)^{1/2}$ at 29 and 127°C.

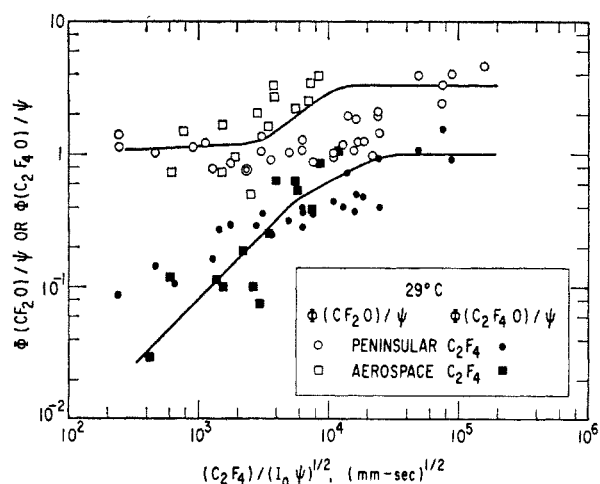


Figure 4. Log-log plots of $\Phi(\text{CF}_2\text{O})/\psi$ and $\Phi(\text{C}_2\text{F}_4\text{O})/\psi$ vs. $(\text{C}_2\text{F}_4)/I_a^{1/2}$ at 29°C.

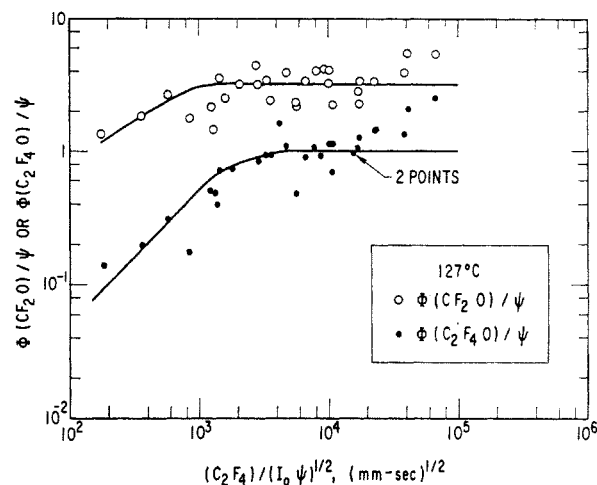


Figure 5. Log-log plots of $\Phi(\text{CF}_2\text{O})/\psi$ and $\Phi(\text{C}_2\text{F}_4\text{O})/\psi$ vs. $(\text{C}_2\text{F}_4)/I_a^{1/2}$ at 127°C.

sumption is justified, and reactions p, q, and r play competing roles.

Figures 4 and 5 present plots of $\Phi(\text{CF}_2\text{O})/\psi$ and $\Phi(\text{C}_2\text{F}_4\text{O})/\psi$ vs. $(\text{C}_2\text{F}_4)/I_a^{1/2}$. The data are badly scattered, but the trends predicted by eq 12 through 15 are evident. The large scatter can be attributed to three causes. First, the experimental determination of $\text{C}_2\text{F}_4\text{O}$ for $\Phi(\text{C}_2\text{F}_4\text{O})$ less than 0.1 is extremely difficult because of the low intensity of the 6.22- μ band of $\text{C}_2\text{F}_4\text{O}$ and the inhibition of $\text{C}_2\text{F}_4\text{O}$ as products accumulate. An experimental error of a factor of 2 is not unlikely. Second, the points which deviate most from the curves are those corresponding to low values of ψ , where the correction factors are of most importance. This is particularly true at high $(\text{C}_2\text{F}_4)/I_a^{1/2}$. Finally, some of the scatter can be attributed to the fact that reactions q and r were neglected in the analysis. Nevertheless, estimates of appropriate rate constant ratios can be made.

From the figures and eq 12, k_n/k_o is found to be about 1.1 at both temperatures. In a study of the reaction of oxygen atoms with C_2F_4 in the presence of O_2 ,⁸ k_n/k_o was found to be 1.1 at 125° and 0.55 at 23°. In that study, the room temperature value was computed by subtracting two similar numbers, so that the uncertainty was large. In view of the scatter in this study, the agreement between the two studies is quite satisfactory.

From Figures 4 and 5 and eq 15, a lower limit to $k_o/k_p^{1/2}$ can be found. The intercept of the portion of the $\text{C}_2\text{F}_4\text{O}$ curve with unit slope gives a lower limit of $k_o/(2k_p)^{1/2}$. That this is a lower limit is due to the neglect of reactions q and r. Thus $k_o/k_p^{1/2} \geq 1.1 \times 10^{-4} (\text{mm sec})^{-1/2}$ at 29° and $\geq 7.0 \times 10^{-4}$

Table III: Rate Constant Data

Ratio	Value	Units	Source	Comments
k_a/k_c	5×10^{-3}	mm ⁻¹	Eq 1	From upper limit of $\Phi(\text{cyclo-C}_3\text{F}_6)$
	100	M ⁻¹	Eq 1	From upper limit of $\Phi(\text{cyclo-C}_3\text{F}_6)$
k_n/k_b	100	M ⁻¹	Ref 3	...
k_e/k_m	2.8	None	Ref 5, 14-18	See Discussion
k_i/k_l	~0.08	None	...	Best fit of data
k_j/k_1	5.0	mm	Eq 6, Figure 2	From data of ref 2
	2.2×10^{-4}	M	Eq 6, Figure 2	From data of ref 2
k_n/k_o	1.1	None	Eq 12, Figures 4, 5	...
	1.1 ^a	None	Ref 8	...
$k_o/k_p^{1/2}$	0.55 ^b	None	Ref 8	...
	$\geq 1.1 \times 10^{-4c}$	(mm sec) ^{-1/2}	Eq 15, Figure 4	...
	$\geq 0.015^c$	(M sec) ^{-1/2}	Eq 15, Figure 4	...
	$\geq 0.098^b$	(M sec) ^{-1/2}	Ref 8	...
	$\geq 7.0 \times 10^{-4d}$	(mm sec) ^{-1/2}	Eq 15, Figure 5	...
	$\geq 0.11^d$	(M sec) ^{-1/2}	Eq 15, Figure 5	...
k_q/k_r	~0.2 ^a	(M sec) ^{-1/2}	Ref 8	...
	~1	None	Eq 16, Figures 4, 5	...
$k_o k_g^{1/2}/(k_q + k_r)$	$\geq 0.8 \times 10^{-4c}$	(mm sec) ^{-1/2}	Eq 17, Figure 6	...
	$\geq 0.011^c$	(M sec) ^{-1/2}	Eq 17, Figure 6	...
	$\geq 6.0 \times 10^{-4d}$	(mm sec) ^{-1/2}	Eq 17, Figure 6	...
	$\geq 0.095^d$	(M sec) ^{-1/2}	Eq 17, Figure 6	...

^a At 125°. ^b At 23°. ^c At 29°. ^d At 127°.

(mm sec)^{-1/2} at 127°. The values found for this ratio in ref 8 were 7.2×10^{-4} and about 13×10^{-3} (mm sec)^{-1/2} at 23 and 125°, respectively. Thus the lower limits found here lie close to but below those found previously. The obvious conclusion is that reactions q and r play an important role in the mechanism.

If we ignore reaction p, then the importance of (q) and (r) can be estimated from eq 16 and 17 and Figure 6. If (p) is negligible, then k_q should be similar to k_r to satisfy (16) and the fact that $\Phi(\text{CF}_2\text{O})/\psi$ approaches a lower limit of unity. However, since (p) is not negligible, this conclusion is quite crude.

Figure 6 is log-log plot based on eq 17. The scatter in the data is similar to that in Figures 4 and 5 for similar reasons [reaction p neglected rather (q) and (r)]. From the intercepts of the portion of the curves with unit slope, a lower limit to $k_o k_g^{1/2}/(k_q + k_r)$ can be estimated. Again, only a lower limit is obtained because reaction p was neglected. Thus $k_o k_g^{1/2}/(k_q + k_r) \geq 0.8 \times 10^{-4}$ (mm sec)^{-1/2} at 29° and $\geq 6.0 \times 10^{-4}$ (mm sec)^{-1/2} at 127°.

Finally, we wish to comment on the absence in this system of the branched-chain mechanism or the marked acceleration that was observed at 125° in our study of the reaction of oxygen atoms with C₂F₄ in the

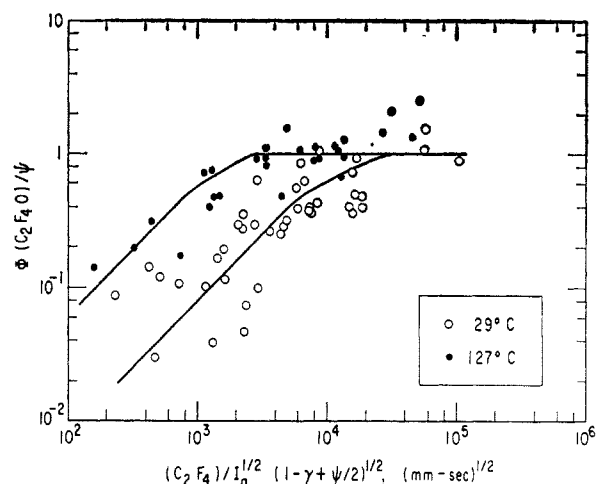


Figure 6. Log-log plots of $\Phi(\text{C}_2\text{F}_4\text{O})/\psi$ vs. $(\text{C}_2\text{F}_4)/I_a^{1/2}(1-\gamma+\psi/2)^{1/2}$ at 29 and 127°.

presence of O₂. It seems to us that this discrepancy reflects a temperature difference in the two systems, even though both high temperatures are reported to be the same. The two studies were done in different vacuum systems with different reaction cells. The thermocouple was placed at the intersection of the stem

and the cross. However, most of the reaction occurs near the stem window, and perhaps the temperature there was several degrees higher in our previous study or several degrees lower in this study, or both. The branched-chain step should be markedly temperature dependent, and a temperature difference of several degrees could have a profound effect. The supposition that the effective temperature was less than 127° in this study is supported by an examination of the cyclo-C₃F₆ data. As explained earlier, our results in Figure 1 should lie below those of Cohen and Heicklen³ because of the differences in cell shape in the respective systems. However, at room temperature, our results are only 30% below Cohen and Heicklen's, whereas at 127° they are almost a factor of 2.5 lower. This excessive lowering would be expected if in fact the effective temperature in this study were less than

127°. Fortunately, all other rate constants are nearly temperature independent. Thus, even if the high temperatures are somewhat in error, the effect on those rate constants would be negligible.

V. Summary

A reasonable and consistent mechanism is given by reactions a through r. A number of rate constant ratios could be ascertained, and they are tabulated in Table III along with literature values where available. The ratios obtained all seem reasonable and compare favorably with previous estimates.

Acknowledgment. The authors wish to thank Mr. Dennis Saunders for preparation of the Aerospace C₂F₄ and Mrs. Barbara Peer for assistance with the manuscript. This research was supported by the U. S. Air Force under Contract No. AF 04(695)-669.